Cross-Dehydrogenative Couplings between Indoles and β-Keto Esters: Ligand-Assisted Ligand Tautomerization and Dehydrogenation via a Proton-Assisted Electron Transfer to Pd(II)

Mikko V. Leskinen,[†] Ádám Madarász,[‡] Kai-Tai Yip,[†] Aini Vuorinen,[†] Imre Pápai,*,[‡] Antti J. Neuvonen,[†] and Petri M. Pihko*,[†]

[†]Department of Chemistry and NanoScience Center, University of Jyväskylä, FI-40014 Jyväskylä, Finland
[‡]Research Center for Natural Sciences, Hungarian Academy of Sciences, Magyar Tudosok Korutja 2, H-1117, Budapest, Hungary

Ⓢ Supporting Information

ABSTRACT: Cross-dehydrogenative coupling reactions between β-ketoesters and electron-rich arenes, such as indoles, proceed with high regiochemical fidelity with a range of β-ketoesters and indoles. The mechanism of the reaction between a prototypical β-ketoester, ethyl 2-oxocyclopentanonecarboxylate, and N-methylindole has been studied experimentally by monitoring the temporal course of the reaction by ^{1}H NMR, kinetic isotope effect studies, and control experiments. DFT calculations have been carried out using a dispersion-corrected range-separated hybrid functional (ωB97X-D) to explore the basic elementary steps of the catalytic cycle. The experimental results indicate that the reaction proceeds via two catalytic cycles.

Cycle A, the dehydrogenation cycle, produces an enone intermediate. The dehydrogenation is assisted by N-methylindole, which acts as a ligand for Pd(II). The computational studies agree with this conclusion, and identify the turnover-limiting step of the dehydrogenation step, which involves a change in the coordination mode of the β-keto ester ligand from an O,O'-chelate to an α-C-bound Pd enolate. This ligand tautomerization event is assisted by the π-bound indole ligand. Subsequent scission of the β'-C—H bond takes place via a proton-assisted electron transfer mechanism, where Pd(II) acts as an electron sink and the trifluoroacetate ligand acts as a proton acceptor, to produce the Pd(0) complex of the enone intermediate. The coupling is completed in cycle B, where the enone is coupled with indole. Pd(TFA)$_2$ and TFA-catalyzed pathways were examined experimentally and computationally for this cycle, and both were found to be viable routes for the coupling step.
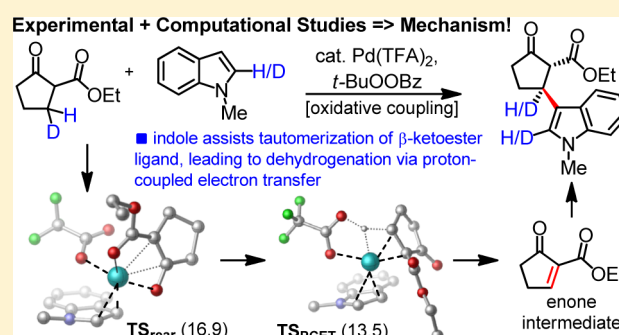
INTRODUCTION

Dehydrogenative cross-couplings, or cross-dehydrogenative couplings between two partners with C—H bonds, constitute an attractive strategy in chemical synthesis.[1] In particular, when the reaction partners include sp[3] C—H bonds, the reactions can be used to generate molecular complexity in three dimensions, and at the same time allow functionalization in remote positions. Although there have been significant advances in this field in recent years,[2,3] dehydrogenative functionalization reactions involving remote sp[3] C—H groups are still rare.[4] In part, this might be due to the fact that the mechanisms of dehydrogenative cross-couplings are only partially understood.

Herein, we present a full account on the mechanistic investigation and the scope of the selective Pd(II)-catalyzed dehydrogenative cross-coupling reaction between indoles and β-keto esters.[5] This reaction is an example of a cross-dehydrogenative coupling between sp[3] and sp[2] C—H bonds. Besides indoles, the reaction also accepts electron-rich aromatics and phenols as the coupling partner[6] and also allows for a three-component coupling between arylboronates, indoles, and β-keto esters (Scheme 1).[7]

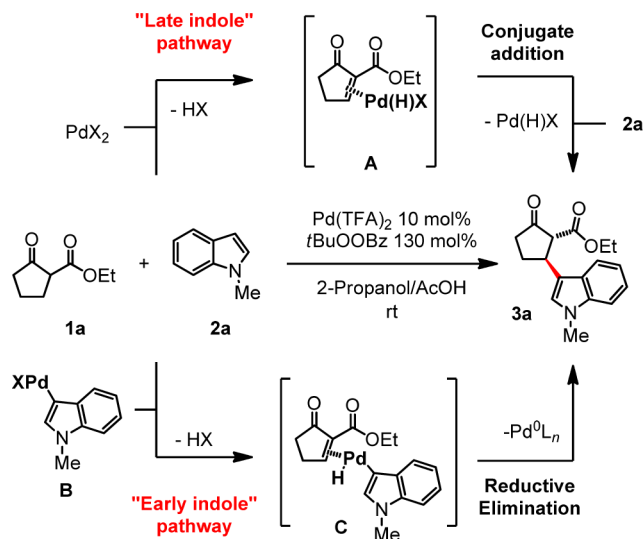**Scheme 1. Development of Dehydrogenative β'—C(sp^3)—H C(sp^2)—H Coupling Reaction**
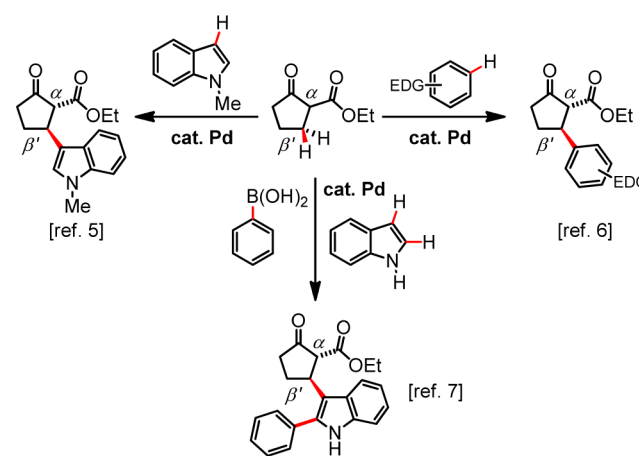
■ RESULTS AND DISCUSSION

In our initial communication, we presented two possible mechanistic scenarios for this reaction (Scheme 2). The first, a

Scheme 2. Palladium-Catalyzed Dehydrogenative β′-Functionalization of β-Keto Ester with Indole and Originally Proposed Reaction Mechanism

Figure 1. Monitoring of the temporal progress of the coupling by ^{1}H NMR spectroscopy. Reaction conditions: $[1a]_0 = 0.476$ M, $[2a]_0 = 0.318$ M, $[tBuOOBz]_0 = 0.413$ M, 10 mol % Pd(TFA)$_2$, 4:1 [D$_8$]-dioxane/AcOH, 300 K. The reported rates are averages of three experiments. Rate$_0$ and rate$_{53}$ refer to the initial rate and the rate at $t = 53$ min, respectively.

"late indole", scenario involves a Saegusa oxidation[8] of **1a** to enone intermediate **A** followed by a Friedel−Crafts-type Pd-catalyzed conjugate addition of indole **2a**. The second, an "early indole", scenario starts with the well-established C3-palladation of indole[9] in which a C3-palladated indole species **B** is involved in the dehydrogenation step, followed by reductive elimination. Our early mechanistic investigations[5] could not distinguish between these two mechanistic possibilities. The key initial observations were: (1) Isolated enone **4a** also afforded the coupling product with indole **2a**, at a rate that was comparable to the overall reaction rate, and (2) without indole **2a**, only very slow formation of enone **4a** was observed. These observations suggested that if enone **4a** was an intermediate, its formation might be dependent on the assistance of indole.

In our early studies, the progress of the reaction was monitored by withdrawing aliquots from the reaction mixture.[5] In this work, we envisioned that the use of online NMR methods to monitor the temporal progress of the reaction would be most beneficial to reveal any fleeting intermediates and to allow the simultaneous monitoring of several species, including the oxidant.[10]

Kinetic Studies. Initially, the standard reaction of β-keto ester **1a** with 1-methylindole (**2a**) was monitored by ^{1}H NMR spectroscopy (Figure 1). The results show that [**4a**] builds up and decays during the initial stage of the reaction, and product formation ([**3a**]) follows a sigmoidal curve. The consumption of indole **2a** also plots a reverse sigmoidal curve. These results strongly suggested that enone **4a** is an intermediate, and indeed, the rate of formation of **3a** peaks close to the concentration peak of **4a**.[11] The sigmoidal shape of the curve for [**4a**] is characteristic of a delay caused by the buildup of the intermediate in a consecutive reaction. The initial rate for the consumption of β-keto ester **1a** (-5.7 mM min^{-1}) is also close to the initial rate of the consumption of the oxidizer tBuOOBz (-5.1 mM min^{-1}).
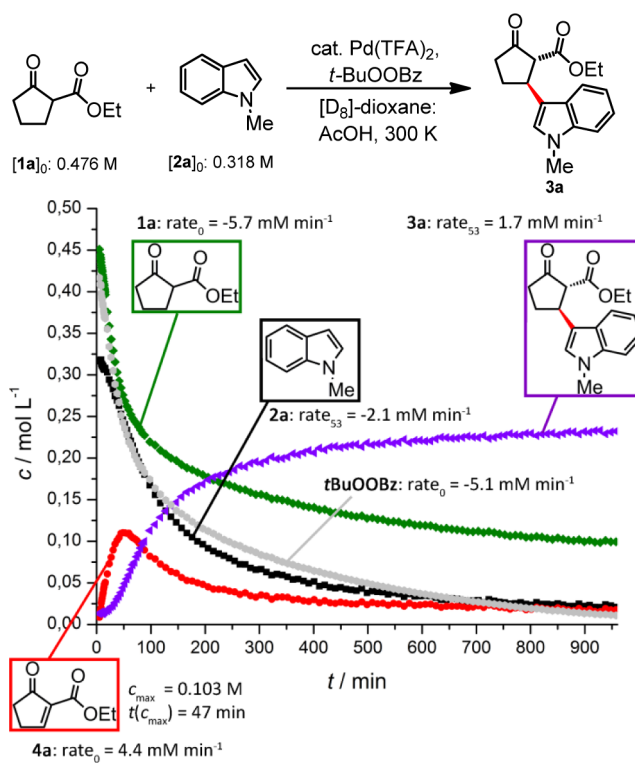
Using separately prepared enone **4a**, the reaction between enone **4a** and indole **2a** was investigated under two sets of conditions. The initial concentration of **4a** was set to 0.12 M, close to the peak concentration of **4a** obtained under the standard oxidative coupling conditions (Figure 1). With Pd(TFA)$_2$ as the catalyst, the reaction between **2a** and **4a** (Scheme 3) progresses at a rate comparable to the peak rate

Scheme 3. Reactions of Indole 2a and Enone 4a
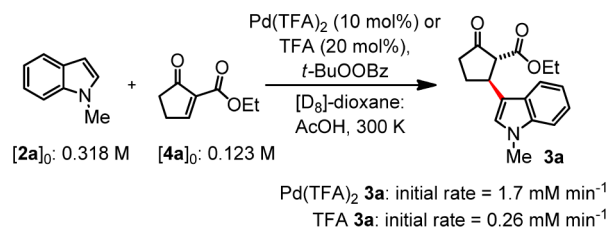
obtained under the standard conditions (1.7 mM min^{-1} for both cases). In contrast, TFA alone as the catalyst allowed the reaction to proceed, but at a significantly slower rate (1.7 mM min^{-1} with Pd(TFA)$_2$ vs 0.26 min^{-1} with TFA, see Scheme 3). These results indicated that Pd(II) also plays a role in the second coupling step, with a possible acid-catalyzed background reaction.

Interestingly, although TFA alone was an inefficient catalyst, the effect of additional TFA to the overall reaction rate was beneficial (Table 1). With added TFA, the reaction proceeded at a reasonable rate even when using Pd(OAc)$_2$ as the Pd(II) source.

Table 1. Effect of TFA on the Reaction Rate[a]
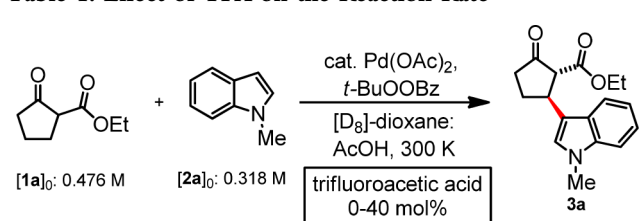
entry	TFA	rate 3a[b] (mM min⁻¹)	rate 4a[c,d] (mM min⁻¹)
1	0 mol %	0.1	0.1
2	10 mol %	1.7	2.9
3	20 mol %	2.3	3.6
4	40 mol %	2.6	3.3

[a]The rates were obtained by monitoring the temporal progress of the coupling by ^{1}H NMR spectroscopy. Reaction conditions: 0−40 mol % TFA, $[\mathbf{1a}]_0$ = 0.476 M, $[\mathbf{2a}]_0$ = 0.318 M, $[t\text{BuOOBz}]_0$ = 0.413 M, 10 mol % Pd(OAc)$_2$, 4:1 [D$_8$]-Dioxane/AcOH, 300 K. [b]Maximum rate [c]Initial rate. [d]In control experiments without Pd(OAc)$_2$ or with Co(OAc)$_2$ (20 mol %) or Fe(OAc)$_3$ (20 mol %), no **4a** or **3a** was produced.

Kinetic Isotopic Effects and Deuterium Labeling. Although the above experiments established that enone **4a** is indeed a viable intermediate for the reaction, control experiments without indole **2a** clearly demonstrated that enone formation is very slow in the absence of indole.[5] The reaction progress method allowed us to obtain kinetic isotope effect (KIE) data for all key reaction components using deuterium-labeled starting materials.[12]

The first KIE experiment involved a comparison of C2-H vs C2-D-labeled indole (Figure 2a).[13] All reaction components displayed significant inverse KIEs in this experiment (Figure 2). These results indicate that **D-2a** accelerates the formation of the enone **4a**. The increased rate of product formation (**3a**) might be due to increased rate of the formation of the intermediate.

A second set of KIE experiments were conducted with deuterium-labeled β-keto ester **D$_6$-1a** (Figure 2b). In this case, unfortunately, the formation of the corresponding enone could not be reliably monitored. Although the rate of consumption of **D$_6$-1a** appears to display an inverse KIE, possible initial H/D exchange or differences in the rates of the formation of the Pd(II) complexes of **1a** could also account for this observation. Indeed, the overall rate of the reaction did not exhibit any KIE (**3a**: k_H/k_D = 0.98), and the initial rate of the consumption of the oxidant indicated a small normal KIE (k_H/k_D = 1.07). Because the consumption of the oxidant is most likely correlated with the concentration of the enone **4a**, these results suggest that the dehydrogenative reaction that produces **4a** is unlikely to exhibit a KIE, although this step must involve the breaking of the β′-H bond of **1a**.

Competition Studies. To obtain further insight into the reaction mechanism, the KIEs were also assayed via competition studies.[12] As shown in Scheme 4, an intermolecular competition reaction between substrates **2a** and **D-2a**, starting with **1a**, gives a product distribution P$_H$/P$_D$ 1:1.22. If **2a** is not dissociated from Pd after the first stage of the reaction (formation of enone **4a**), then the observed KIE could be explained by the more rapid rate of enone formation with **D-2a**. However, the fact that a significant concentration of free enone can be observed during the reaction (Figure 1) suggests that the catalytic cycle responsible for the coupling of enone **4a** and
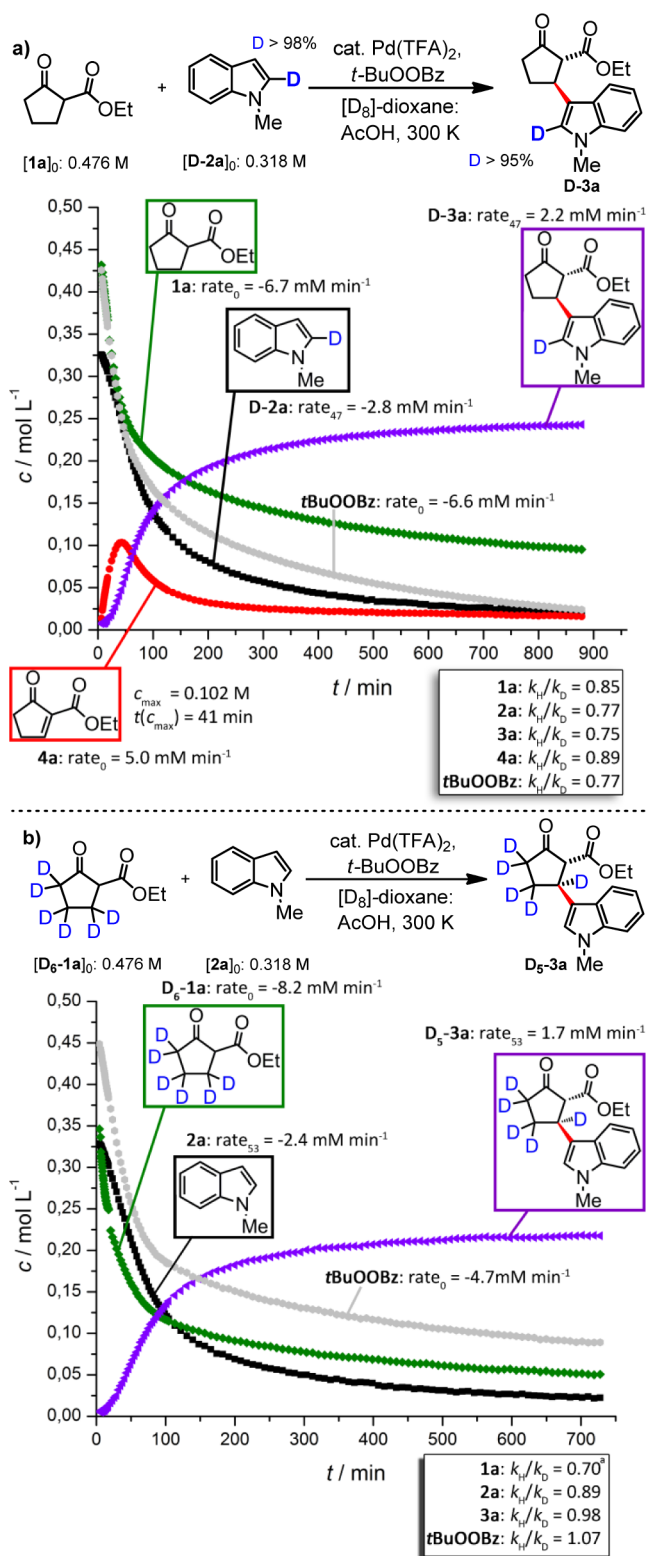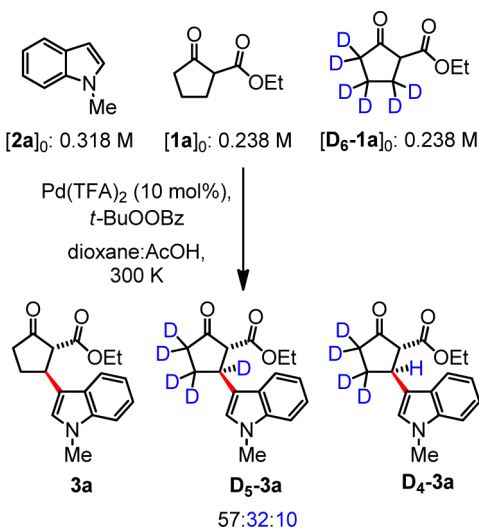

Figure 2. Temporal progress of the coupling by ^{1}H NMR spectroscopy with deuterated starting materials. Reaction conditions: (a) $[\mathbf{1a}]_0$ = 0.476 M, $[\mathbf{D\text{-}2a}]_0$ = 0.318 M, (b) $[\mathbf{D_6\text{-}1a}]_0$ = 0.476 M, $[\mathbf{2a}]_0$ = 0.318 M. For both experiments: $[t\text{BuOOBz}]_0$ = 0.413 M, 10 mol % Pd(TFA)$_2$, 4:1 [D$_8$]-Dioxane/AcOH, 300 K. Rates and k_H/k_D are averages of three experiments (a) or two experiments (b). Rate$_0$ and rate$_{xx}$ refer to the initial rate and the rate at t = xx min, respectively.

Scheme 4. Competition Studies between 2a and D-2a

**Scheme 5. Intermolecular Competition between D_6-1a and 1a in the Coupling Process**
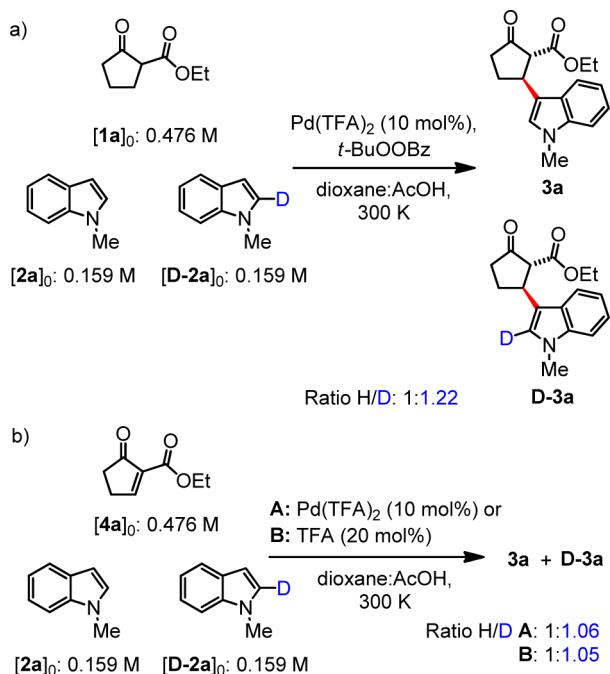
indole **2a** is at least partially separated from the first dehydrogenation cycle that produces enone **4a**. Therefore, the observed KIE in Scheme 4a could be related to the C−C formation step. To assay this possibility, intermolecular competition experiments with **2a** and **D-2a** were conducted using enone **4a** as the substrate. These experiments gave a P_H/P_D that was much closer to unity under both Pd(II) catalysis and TFA catalysis (Scheme 4b), suggesting that the KIE observed with **1a** (Scheme 4a) originates from the dehydrogenation step and that **4a** may not be fully dissociated from the Pd complex that eventually leads to the product **3a**.

In the competition reaction between **1a** and D_6-**1a**, the nondeuterated **1a** reacts faster than the deuterated D_6-**1a** (Scheme 5). This result is in agreement with the small normal KIE observed for oxidant consumption with D_6-**1a** in the

parallel experiment (Figure 2b), suggesting that D_6-**1a** is dehydrogenated at a slower rate than **1a**. Interestingly, some H/D exchange appears to take place in this experiment, producing D_4-**3a** (Scheme 5).

Finally, in an *intra*molecular competition experiment, the mono-β'-deuterated D_1-**1a** gave rise to product **3a** that exhibited a 48.6:51.4 H/D ratio (Scheme 6). The absence of a KIE in this experiment suggests that the β'-H bond cleavage is not turnover-limiting for the dehydrogenation cycle (see below for further discussion).

Scheme 6. Intramolecular Competition Studies with β'-Monodeuterated D_1-1a
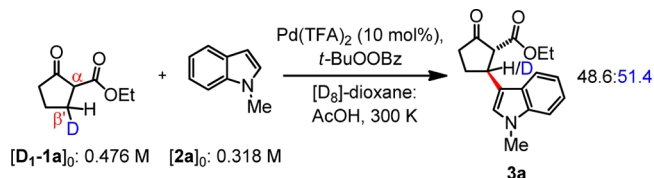
The effect of the electron-withdrawing alkyl ester was studied using β-keto ester **1b**. Under the standard conditions, the reaction between **1b** and **2a** was significantly slower than the standard reaction between **1a** and **2a** (0.52 mM min^{-1} with **1b** vs 1.7 mM min^{-1} with **1a**). This rate difference was also confirmed by an intermolecular competition between **1a** and **1b** (P_{3a}/P_{3b} value of 3, see Scheme 7). These rates reflect the measured rates of the dehydrogenation step (rate of formation of enone: 1.6 mM min^{-1} for the enone derived from **1b**, vs 4.4 mM min^{-1} for **4a**).[14]

**Scheme 7. Intermolecular Competition between 1a and 1b in the Coupling Process**
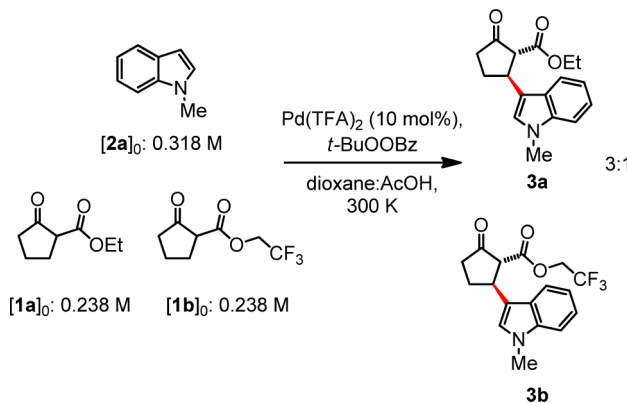
In summary, these kinetic experiments revealed that (1) the reaction likely proceeds in two stages, via an enone intermediate (**4a**), (2) the formation of enone is dependent on indole, and (3) the C−C bond formation step can proceed under both acid catalysis as well as under Pd(II) catalysis. In parallel with these experiments, the intimate details of the mechanism were subjected to a computational study.

Computational Studies and Revision of the Mechanism. Based on our experimental findings, we envisioned that the Pd-catalyzed dehydrogenative cross-coupling reaction between β-ketoester **1a** and indole **2a** takes place via two distinct catalytic cycles (Scheme 8) corresponding to the formation of the enone intermediate (cycle A) followed by the
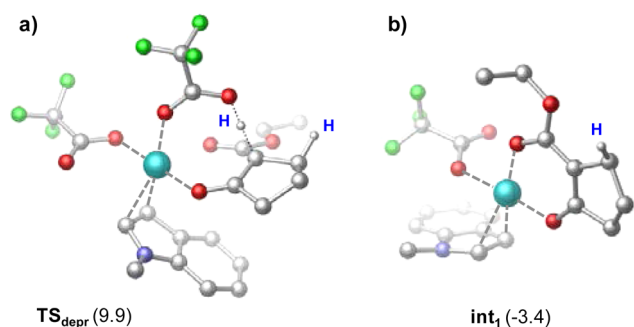
Scheme 8. Schematic View of Catalytic Cycles for the Dehydrogenation and the C−C Bond Formation Steps
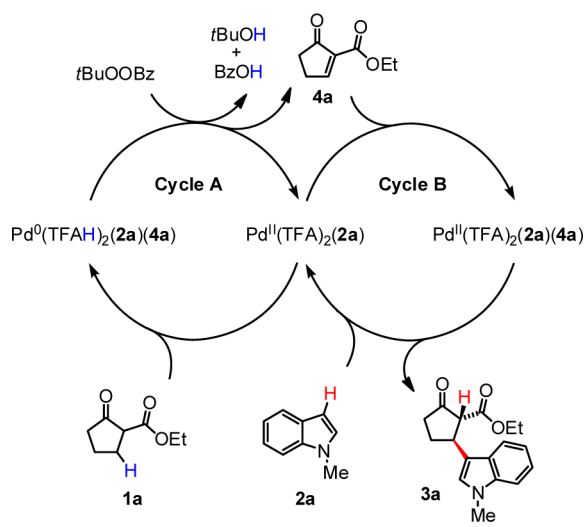
C−C bond formation process with indole (cycle B). As indicated in Scheme 8, the Pd(TFA)$_2$(2a) species may represent a common intermediate of the two cycles. We carried out DFT calculations with the main aim at identifying and characterizing the key elementary steps of these cycles.[15]

Dehydrogenation: Cycle A. In accordance with previous studies on Pd-catalyzed dehydrogenation reactions, we considered a sequence of C−H-activation/β-hydride elimination steps in cycle A. The assistance of indole was clearly demonstrated in our experiments; therefore, we assumed that 2a acts as a coligand along the entire reaction pathway.

The calculations indicate that the deprotonation of 1a at the α-carbon atom can occur easily via a tetracoordinate Pd(II) complex involving two TFA ligands and both substrates bound to the metal center (intermediate Pd(TFA)$_2$(1a)(2a)). This complex is predicted to be at −0.1 kcal/mol with respect to Pd(TFA)$_2$(2a) + 1a.[16] The transition state identified for the deprotonation is depicted in Figure 3a and it represents only a small activation barrier (9.9 kcal/mol). It is apparent that the C−H bond of 1a is activated by a neighboring TFA ligand resulting in a Pd-enolate intermediate, which is stabilized by the dissociation of the TFAH molecule. This latter reaction intermediate (int$_1$ in Figure 3b) lies slightly below the

reference level (at −3.4 kcal/mol), and it is characterized by chelating coordination of the enolate ligand through the two carbonyl moieties ($\eta^2(O,O')$ complex).[17]

For the β-hydride elimination step, the β′-hydrogen should be accessible by the metal center, therefore, ligand rearrangement is expected as a next step along the reaction pathway. The simplest transformation would be an internal rearrangement of the bonding between Pd and enolate preserving the same stoichiometry, but other pathways (including various dissociation/association steps) are also feasible. Our attempts to explore these transformations pointed to several transition states lying higher in free energy than TS$_{depr}$. For instance, the transition state connecting int$_1$ with an η^3-Pd-enolate intermediate (i.e., displacement of the ester group from the coordination sphere, see TS$_{rear}$ and int$_2$ in Figure 4) is predicted to be at 16.9 kcal/mol, giving rise to a barrier of 20.3 kcal/mol (relative to int$_1$).[18]
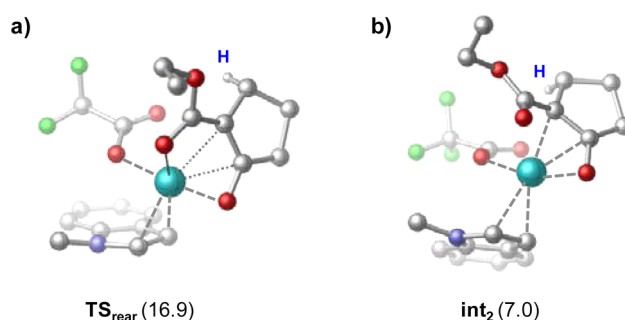
Figure 4. Decoordination of the ester group in intermediate int$_1$: (a) transition state (b) product state of rearrangement.

Additional ligand rearrangement can lead to an intermediate involved directly in the β-hydride elimination step (see int$_3$ in Figure 5). In this species, the enolate is bound covalently to Pd via the α-carbon atom ($\eta^1(C)$ complex) and it displays characteristic β-agostic interactions with the metal center.

Figure 5. The proton-coupled electron transfer (PCET) transition state of cycle A and the corresponding reactant and product state intermediates.

Figure 3. Transition state located for the substrate deprotonation step of cycle A (a) and the corresponding product state intermediate (b). Relative Gibbs free energies (in kcal/mol, with respect to Pd-(TFA)$_2$(2a) + 1a) are shown in parentheses. Metal−ligand bonds are indicated by dashed lines. For clarity of figures, hydrogen atoms are omitted, except those involved in dehydrogenation.
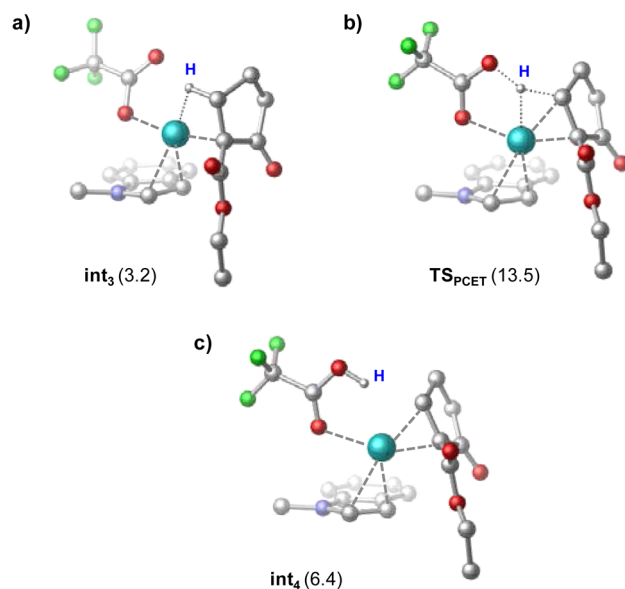
This complex is computed to be at +3.2 kcal/mol on the free energy scale. Surprisingly, the Pd-mediated C−H bond cleavage does not yield the expected palladium-hydride species because the located transition state (**TS**$_{PCET}$ in Figure 5) describes a direct hydrogen migration to the free oxygen of the TFA ligand without the formation of a palladium-hydride intermediate (PdH species could only be identified computationally as very unstable structures).[11]

The population analysis carried out for the transition state and the corresponding intermediates reveals that this elementary step can be characterized as a concerted proton-coupled electron transfer (PCET) process involving proton migration to TFA occurring in concert with 2e⁻ electron transfer to the metal center.[19,20] This reaction step results in a Pd(0)(TFAH)(**2a**)(**4a**) complex as an intermediate (**int**$_4$ in Figure 5) lying at 6.4 kcal/mol. The computed activation barrier of the PCET step is 16.9 kcal/mol with respect to the low-lying **int**$_1$ intermediate, that is, much lower than that of the ligand rearrangement step (20.3 kcal/mol, **TS**$_{rear}$ with respect to **int**$_1$). After this step, the catalytic cycle involves the oxidation of Pd(0) and the elimination of the enone molecule. These transformations were not examined computationally in the present work.

The Gibbs free energy diagram of the reaction route explored for the dehydrogenation process is depicted in Figure 6. These
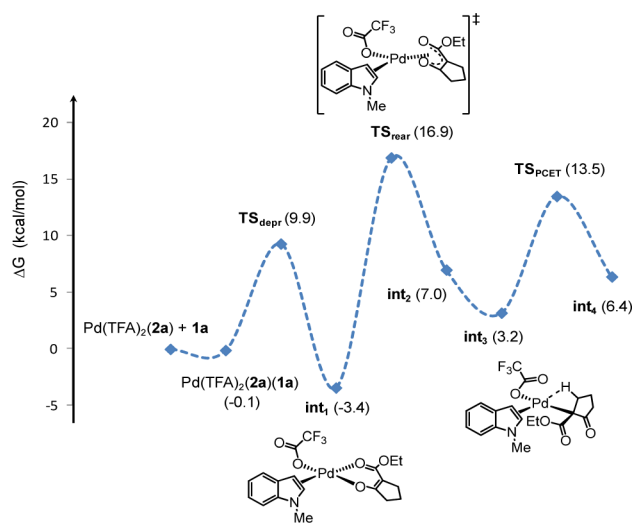
Figure 6. Gibbs free energy diagram computed for the dehydrogenation process.

results point toward a reasonable mechanism for the dehydrogenation process, however, they indicate that the $\eta^2(O,O')$ to $\eta^1(C)$ rearrangement of the enolate ligand, and not the PCET step, might be rate-determining in cycle A.

Indole-Assisted Dehydrogenation. To assess the role of indole in the dehydrogenation cycle, we examined analogous reaction pathways using a model with a TFAH coligand replacing the indole. We find that the activation barriers are notably higher than those presented above. The largest difference was obtained for the ester decoordination step (the barrier increased to 24.2 kcal/mol), indicating that indole coordination is clearly beneficial in terms of the reaction rate. Interestingly, the PCET mechanism of C−H bond cleavage is maintained in the absence of indole as well, although the barrier of this step is predicted to be slightly higher in this case (15.0 kcal/mol).

To rationalize the results of KIE experiments with **2a**, we calculated the KIE values based on the relative barriers with the different isotopomers of **2a**. With **D-2a**, the calculated KIE is 0.85 considering that **TS**$_{rear}$ is the turnover-determining transition state.[12,21] The calculated value is very close to the experimental KIE (0.77−0.85, see Figure 2). The magnitude of the KIE is similar to cases where hybridization changes from $C(sp^2)$ to $C(sp^3)$,[22] suggesting that the steric environment of C2 of **2a** becomes significantly more crowded in the turnover-determining transition state **TS**$_{rear}$ compared to the turnover-determining intermediate. This result suggests that **2a** assists the tautomerization step by coordinating more tightly (primarily via its 2,3-π-bond) to Pd(II) in the transition state **TS**$_{rear}$. Indeed, computations indicate that the bond distance between the C2 atom of the coordinated indole and the Pd atom is considerably shortened in the **TS**$_{rear}$ compared to the related reactant state (**int**$_1$) (the computed Pd−C2 bond lengths are 2.28 and 2.34 Å, respectively). The need for indole assistance in this step may result from increased electron deficiency of the Pd(II) center in **TS**$_{rear}$ due to decoordination of **1a**.

To test this hypothesis, we also experimentally explored other electron-rich ligands which would not react with **4a** but would nevertheless be able to withstand the oxidative conditions. In addition to sulfoxides (DMSO and PhSOMe),[23] 1,2,3-trimethylindole and 1,3-dimethylindole were able to significantly accelerate the dehydrogenation step (see the Supporting Information).[11]

If the PCET step, where the β'-H bond is cleaved, would be the turnover-determining step in cycle A, a much larger KIE would be expected than that observed experimentally with β'-deuterated **1a** variants (the experimental KIE is close to 1, see Figure 3 and Scheme 6). The calculated KIE for the PCET step is quite large (7.06), and it is in sharp contrast with the value obtained from the intramolecular competition experiment (Scheme 6), which is expected to be most sensitive to any KIE in the product-determining step. The fact that no primary KIE is observed even under these conditions can be rationalized by considering that the different hydrogen isotopes are *not* in an equal environment after the turnover-limiting step (i.e., **TS**$_{rear}$).[24] The choice between β'-H vs β'-D abstraction has already been made in the turnover-determining ligand rearrangement step which leads to the formation of C-bound enolate **int**$_3$. The effect of deuterium substitution in the β' position of the ligand on the ligand rearrangement step is expected to be small, resulting in a negligible primary KIE.

The finding that the turnover is determined by the ligand tautomerization step (from a O,O'-chelate **int**$_1$ to C-bound **int**$_3$) is interesting. α-Substituted β-dicarbonyl compounds are known to be unproductive in α-arylation reactions,[25] and our results suggest that such low reactivity might have a kinetic origin. Specifically, if the barrier for the formation of the C-bound enolate from the O,O'-chelate intermediate is too high, this would prevent *both* dehydrogenation and α-arylation reactions. In a control experiment, methyl dimethylmalonate (**5**), a very sluggish substrate for α-arylation,[25a] failed to give any coupling products with **2a** under the standard reaction conditions (eq 1).[11]

This result could be rationalized by the higher Lewis basicity of the ester oxygens in **5**, which might result in a O,O'-chelated intermediate that would be too stable to undergo the tautomerization to the C-bound enolate. Because ligands such as indole are able to assist the tautomerization step, we can
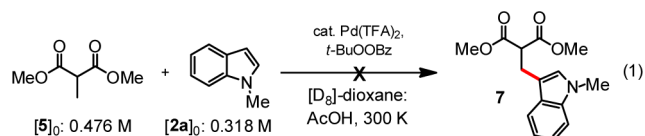
speculate that perhaps more efficient π-donor ligands might overcome these limitations.

The C−C Coupling Process. According to the experimental evidence, the C−C coupling process (cycle B) could proceed either via acid catalysis or Pd(II) catalysis under acidic conditions. The reaction between **2a** and **4a** could conceivably take place via either Lewis acid catalysis (Pd^{2+}), C-palladation of **2a**, or Brønsted acid catalysis, among other possibilities. We therefore examined these reaction routes computationally, and plausible pathways were identified for these scenarios. For brevity, herein we discuss only the C-palladation mechanism in detail, which is predicted to have the lowest activation barrier among the investigated pathways. The alternative pathways are presented in the Supporting Information.[11]

The C-palladation pathway begins with the formation of a Pd(TFA)$_2$(**2a**)(**4a**) complex, which involves both coupling partners (indole **2a** and enone **4a**). Although this complex lies fairly high in free energy (11.8 kcal/mol with respect to Pd(TFA)$_2$(**2a**) + **4a**), it can undergo C−H activation (concerted metalation-deprotonation)[26] via transition state **TS$_{CH}$** to yield intermediate **int$_{CH}$** (Figure 7). The located
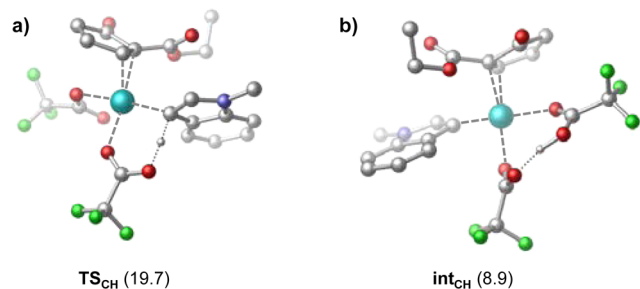

Figure 7. C−H activation of indole **1a**.

transition state is computed to be at 19.7 kcal/mol, and the resulting intermediate is predicted to be at 8.9 kcal/mol. In **int$_{CH}$**, the indole is covalently bound to Pd, whereas enone **4a** is π-coordinated.

Facile C−C bond formation may take place from **int$_{CH}$** (Figure 8). The located transition state (**TS$_{CC}$**) lies notably lower in free energy than **TS$_{CH}$**. The product state of the coupling process (**int$_{CC}$**) is a very stable species, wherein the adduct **3a** is bound by multiple bonds to the metal center.
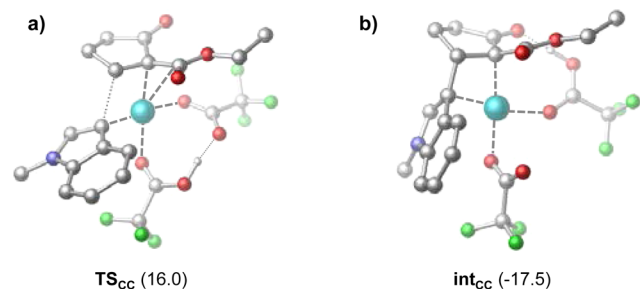

Figure 8. Pd-catalyzed C−C coupling via a C3-palladated indole species.

Protonation of the carbonyl oxygen followed by the dissociation of the enolic form of the product is found to be a reasonable scenario for the completion of the cycle, but other product elimination routes may exist too.

It should be emphasized that the alternative C−C bond formation mechanisms cannot be entirely ruled out either. For example, for a Brønsted acid catalyzed pathway (TFA as the catalyst), calculations predict a barrier very similar to that obtained for the C-palladation pathway (19.9 kcal/mol). Furthermore, a Lewis acid catalyzed pathway, involving Pd^{2+}, was found to have a slightly higher barrier (22.3 kcal/mol).[11] Although there are close literature precedents involving Pd^{2+} as a Lewis acid in Friedel−Crafts reactions between indoles and α,β-unsaturated carbonyl compounds,[27] it should be noted that the reaction conditions (aprotic solvents, such as CH$_2$Cl$_2$ and noncoordinating counterions, such as SbF$_6^-$) are quite different to those studied here (trifluoroacetate counterions, polar/protic solvent).

Resting State of the Catalyst. Although the computations give reasonable barriers for the C−C bond forming step starting from Pd(TFA)$_2$, the stability of the product complex **int$_{CC}$** suggests that recycling Pd(II) requires further assistance, for example, from the acidic solvent or β-ketoesters. We were able to crystallographically characterize a dinuclear [Pd$_2$(TFA)$_2$(**3a**)$_2$] complex from a reaction conducted with 100 mol % of Pd(TFA)$_2$.[11,28] In this complex, **3a** is a bidentate ligand for Pd(II), with a binding geometry that is strikingly similar to **int$_{CC}$**. This complex could also be characterized computationally, and the experimentally and computationally derived structures are presented in Figure 9. The isolability of this complex suggests that Pd(II)-**3a** complexes are stable intermediates, and their decomplexation might even limit the turnover of the reaction.
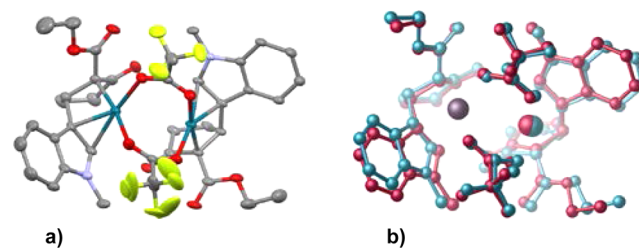

Figure 9. Structure of the Pd$_2$(TFA)$_2$(**3a**)$_2$] complex: (a) X-ray structure, (b) overlay of X-ray (blue) and computed (red) structures.

As a test for this hypothesis, we found that addition of dimethyl methylmalonate **5** (50 mol %) to the reaction mixture results in a marked increase in the rate of formation of both **3a** and **4a** (Scheme 9), pointing toward a possible assistance of **5** in releasing Pd(II).[29] Alternatively, **5** could act as a ligand for dehydrogenation, but we find this scenario less likely as β-ketoester **1a** alone cannot effectively promote the dehydrogenation without the assistance from indole.[5] We cannot, however, rule out a third possibility that **5** assists in cycle B as a coligand.

Reaction Scope and Asymmetric Variants of the Coupling Reaction. Although clarifying the mechanistic picture of the coupling reaction was the main focus of this study, we also present here the full scope of the transformation and an asymmetric variant of the reaction. As described in our original communication, the reaction readily tolerated electron-rich, electron-poor, and sterically demanding indole-substrates, and both free indole N−H as well as N-methyl and N-benzyl

Scheme 9. Effect of Malonate Ester 5

[1a]$_0$: 0.476 M   [2a]$_0$: 0.318 M

5 (50 mol%)

Rate: 3a: 2.7 mM min^{-1}
4a: 4.9 mM min^{-1}
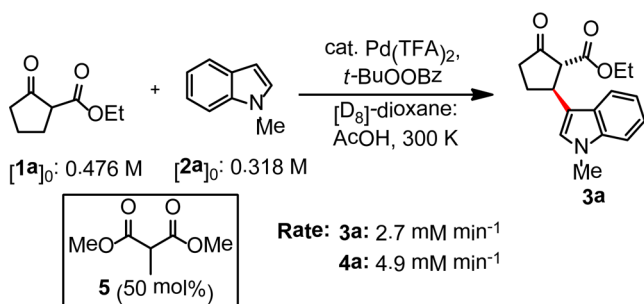
indoles are tolerated. However, sulfonyl or carbamate protecting groups are not tolerated on the indole nitrogen. Furthermore, a range of β-keto esters, including cyclic 5-, 6-, and 7-membered β-keto esters, can be used. Additional substrates that were not described in the initial communication are shown in Scheme 10. The full scope is presented as a Chart in the Supporting Information.

Scheme 10. Additional Substrates for the Indole−β-Keto Ester Oxidative Coupling[a]

3c   96%
3d   83%
3e   70%
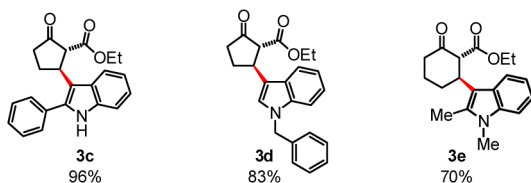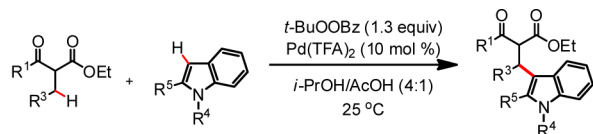
[a]Isolated yields of pure products are reported. Conditions: 1 (1.5 equiv), 2 (0.4 mmol, 1.0 equiv), t-BuOOBz (1.3 equiv), Pd(TFA)$_2$ (0.1 equiv), i-PrOH/AcOH (4:1, 0.5 mL) at 25 °C.
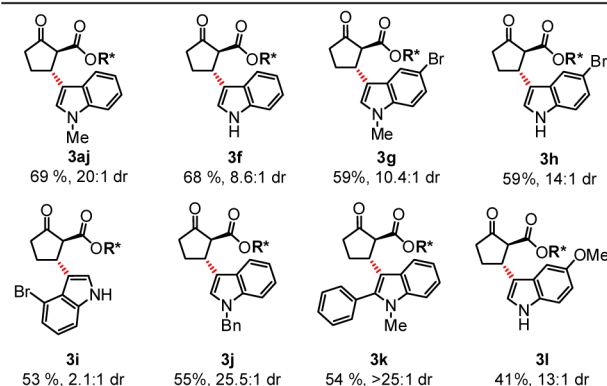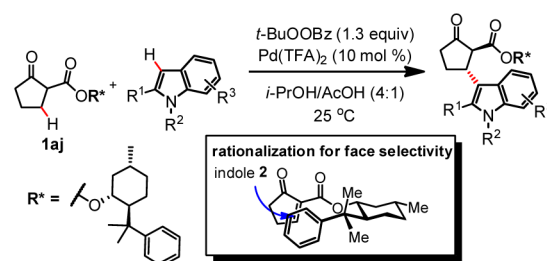
For the development of an asymmetric version of the reaction, we have focused on using a chiral ester auxiliary. Although the use of chiral acids or chiral anions might conceivably induce enantioselectivity via either the Pd(II)- or acid-catalyzed C−C bond formation pathways, our previous experiments with chiral acids and chiral Pd phosphates were not very encouraging.[6] Instead, 8-phenylmenthyl esters[30] exhibited useful levels of diastereoselectivity.[31,32]

Scheme 11 presents the scope of the transformation with different 8-phenylmenthyl β-keto esters. In general, the diastereoselectivities were good. The exception was **3i**, which afforded only moderate 2.1:1 dr. The reaction also tolerates bromine substituents in the indole nucleus (**3g**−**3i**); this is a useful feature for further functionalization of the products. The observed sense of diastereoselection is in full accordance with literature precedents[30] and the model shown in Scheme 11 (inset).

Krapcho decarboxylation of **3aj** provided the corresponding ketone **6** in 62% yield (eq 1) and 98:2 er (eq 2).[11]

■ CONCLUSIONS

β-Keto esters and indoles can be dehydrogenatively cross-coupled with a high regiochemical fidelity under very mild

Scheme 11. Scope of the Diastereoselective Dehydrogenative Coupling with 8-Phenylmenthyl β-Keto Esters[a]

3aj   69 %, 20:1 dr
3f   68 %, 8.6:1 dr
3g   59%, 10.4:1 dr
3h   59%, 14:1 dr
3i   53 %, 2.1:1 dr
3j   55%, 25.5:1 dr
3k   54 %, >25:1 dr
3l   41%, 13:1 dr

[a]Isolated yields of pure products are reported. Conditions, unless otherwise indicated: 1 (1.5 equiv), 2 (0.4 mmol, 1.0 equiv), t-BuOOBz (1.3 equiv), Pd(TFA)$_2$ (0.1 equiv), i-PrOH/AcOH (4:1, 0.5 mL) at rt.

3aj   20:1 dr   6   62%, 98:2 er (GC)   (2)
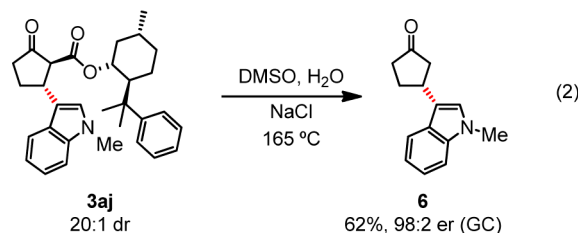
conditions with Pd(II) catalysis. With the combined information obtained from online NMR monitoring experiments, kinetic isotope effects, and computational studies, the previously proposed reaction mechanism was revised. The revised mechanism is presented in Scheme 12.

The reaction involves indole already at the early stage of the catalytic process as a π-bound ligand for Pd(II) that assists the O−to−C tautomerization of β-keto ester **1a**. This is the turnover-determining step of the dehydrogenation cycle. The assistance of indole ligand in the tautomerization step is evident both from the secondary kinetic isotope effects observed for the rate of the dehydrogenation with 2-deuterated N-methylindole and from the computational studies. The dehydrogenation of the β-keto ester is completed by a proton-assisted electron transfer reaction where Pd(II) is simultaneously reduced to Pd(0) and trifluoroacetate ligand accepts a proton from the β′ carbon. No Pd hydride intermediate could be characterized by the computations. For the C−C bond forming step, three plausible pathways involving either acid catalysis or Pd(II) catalysis were identified by computations. Experimentally, Pd(II) was found to accelerate the C−C bond formation, and computationally the most feasible Pd(II)-catalyzed pathway involves the palladation of indole at C3. However, Lewis acid catalysis by Pd^{2+} cannot be excluded. Finally, the synthetic utility of the protocol was expanded to include additional

Scheme 12. Revised Catalytic Cycles
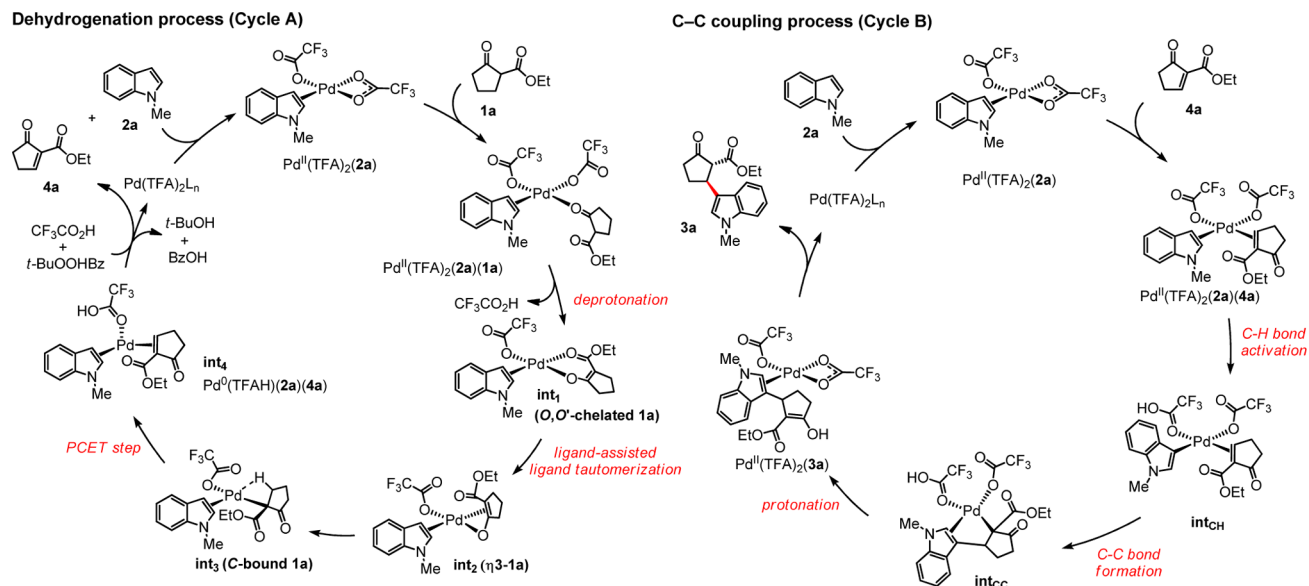
substrates, and an asymmetric version of the reaction could be realized with 8-phenylmenthyl esters.

The reaction between indoles and β-ketoesters appears to be possible only because indoles can serve the double role of a substrate and a ligand in the ligand-assisted tautomerization step, the turnover-determining step of the dehydrogenation cycle. This finding should encourage researchers to look for similar effects in other dehydrogenation and cross-dehydrogenative coupling reactions.

■ ASSOCIATED CONTENT

S **Supporting Information**

Experimental procedures, additional experiments pertaining to the mechanism, characterization data, computational details, and copies of NMR spectra and GC chromatograms. This material is available free of charge via the Internet at http://pubs.acs.org.

■ AUTHOR INFORMATION

Corresponding Author
papai.imre@ttk.mta.hu, petri.pihko@jyu.fi.
Notes
The authors declare no competing financial interest.

■ ACKNOWLEDGMENTS

■ REFERENCES

(1) For review of catalytic dehydrogenative cross-couplings, see: Yeung, C. S.; Dong, V. M. *Chem. Rev.* **2011**, *111*, 1215.

(2) For unselective examples of dehydrogenative arylations of sp³ C—H bonds, see: (a) Deng, G.; Zhao, L.; Li, C.-J. *Angew. Chem., Int. Ed.* **2008**, *47*, 6278. (b) Guo, X.; Li, C.-J. *Org. Lett.* **2011**, *13*, 4977.

(3) For selected reviews of catalytic oxidative functionalizations of sp³ C—H bonds, see: (a) Jazzar, R.; Hitce, J.; Renaudat, A.; Sofack-Kreutzer, J.; Baudoin, O. *Chem.—Eur. J.* **2010**, *16*, 2654. (b) Li, H.; Li, B.-J.; Shi, Z.-J. *Catal. Sci. Technol.* **2011**, *1*, 191. (c) Rouquet, G.; Chatani, N. *Angew. Chem., Int. Ed.* **2013**, *52*, 2. (d) Girard, S. A.; Knauber, T.; Li, C.-J. *Angew. Chem., Int. Ed.* **2014**, *53*, 74.

(4) For intramolecular Pd^II-catalyzed dehydrogenative arylations of sp³ C—H bonds, see: (a) Liègault, B.; Fagnou, K. *Organometallics* **2008**, *27*, 4841. (b) Pierre, C.; Baudoin, O. *Tetrahedron* **2013**, *69*, 4473.

(5) Leskinen, M. V.; Yip, K.-T.; Valkonen, A.; Pihko, P. M. *J. Am. Chem. Soc.* **2012**, *134*, 5750.

(6) Yip, K.-T.; Nimje, R. Y.; Leskinen, M. V.; Pihko, P. M. *Chem.—Eur. J.* **2012**, *18*, 12590.

(7) Nimje, R. Y.; Leskinen, M. V.; Pihko, P. M. *Angew. Chem., Int. Ed.* **2013**, *52*, 4818.

(8) Ito, Y.; Suginome, M. In *Handbook of Organopalladium Chemistry for Organic Synthesis*; Negishi, E.-I., Ed.; Wiley: New York, 2002; Vol. 2, p 2873.

(9) (a) Itahara, T.; Ikeda, M.; Sakakibara, T. *J. Chem. Soc., Perkin Trans. 1* **1983**, 1361. (b) Itahara, T.; Kawasaki, K.; Ouseto, F. *Synthesis* **1984**, 236. (c) Yokoyama, Y.; Matsumoto, T.; Murakami, Y. *J. Org. Chem.* **1995**, *60*, 1486. (d) Jia, C.; Lu, W.; Kitamura, T.; Fujiwara, Y. *Org. Lett.* **1999**, *1*, 2097. (e) Grimster, N. P.; Gauntlett, C.; Godfrey, C. R. A.; Gaunt, M. J. *Angew. Chem., Int. Ed.* **2005**, *44*, 3125. (f) Maehara, A.; Tsurugi, H.; Satoh, T.; Miura, M. *Org. Lett.* **2008**, *10*, 1159.

(10) For examples of online NMR monitoring in detection of several intermediates, see (a) Ref 7. (b) Sahoo, G.; Rahaman, H.; Madarász, Á.; Pápai, I.; Melarto, M.; Valkonen, A.; Pihko, P. M. *Angew. Chem., Int. Ed.* **2012**, *51*, 13144.

(11) See the Supporting Information for details.

(12) (a) Gómez-Callego, M.; Sierra, M. A. *Chem. Rev.* **2011**, *111*, 4857. For an insightful essay, see (b) Simmons, E. M.; Hartwig, J. F. *Angew. Chem., Int. Ed.* **2012**, *51*, 3066.

(13) C3-deuterated **2a** rapidly exchanged the deuterium label with AcOH, with and without Pd(TFA)₂ catalyst. In contrast, the deuterium label at C2 was preserved with **D-2a** under the reaction conditions.

(14) Tanaka, D.; Romeril, S. P.; Myers, A. G. *J. Am. Chem. Soc.* **2005**, *127*, 10323.

(15) Most of the DFT calculations (geometry optimizations, vibrational analysis, estimation of solvent effects) were carried out at ωB97X-D/SDDP level of theory. For each located structure, we carried out additional single-point energy calculations using the same

functional but a larger basis set (supplemented by diffusion functions). The reported energetics refers to relative solution-phase Gibbs free energies. For further details, see Supporting Information.

(16) The Pd(TFA)$_2$(**2a**) + **1a** state was arbitrarily chosen as a reference level for the estimation of relative Gibbs free energies because the experimental evidence indicated involvement of **2a** in the dehydrogenation of **1a**.

(17) For an early review on coordination chemistry of β-dicarbonyl compounds, see Kawaguchi, S. *Coord. Chem. Rev.* **1986**, *70*, 51. For experimental studies of Pd(II) enolates, see: (b) Culkin, D. A.; Hartwig, J. F. *Organometallics* **2004**, *23*, 3398. (c) Wolkowski, J. P.; Hartwig, J. F. *Angew. Chem., Int. Ed.* **2002**, *41*, 4289.

(18) The computed barrier is consistent with those reported for analogous *O*-bound enolate to *C*-bound enolate tautomerization processes of Ni- and Pd-enolate complexes, although the structure of the enolate ligand is different: (a) Cámpora, J.; Maya, C. M.; Palma, P.; Carmona, E.; Gutiérrez, E.; Ruiz, C.; Graiff, C.; Tiripicchio, A. *Chem.—Eur. J.* **2005**, *11*, 6889. (b) Oertel, A. M.; Ritleng, V.; Busiah, A.; Veiros, L. F.; Chetcuti, M. J. *Organometallics* **2011**, *30*, 6495.

(19) For recent comprehensive reviews on proton-coupled electron transfer reactions, see (a) Huynh, M. H. V.; Meyer, T. J. *Chem. Rev.* **2007**, *107*, 5004. (b) Weinberg, D. R.; Gagliardi, C. J.; Hull, J. F.; Murphy, C. F.; Kent, C. A.; Westlake, B. C.; Paul, A.; Ess, D. H.; McCafferty, D. G.; Meyer, T. J. *Chem. Rev.* **2012**, *112*, 4016.

(20) For studies describing metal-catalyzed C−H bond cleavage reactions in terms of the PCET mechanism, see (a) Seu, C. S.; Appel, A. M.; Doud, M. D.; DuBois, D. L.; Kubiak, C. P. *Energy Environ. Sci.* **2012**, *5*, 6480. (b) Nielsen, R. J.; Goddard, W. A., III *J. Am. Chem. Soc.* **2006**, *128*, 9651. Note that in the latter work, this mechanism is referred to as reductive β-hydride elimination. The computed charges of the **int**$_3$, **TS**$_{PCET}$ and **int**$_4$ stationary points indicate that a proton and not a hydridic or radical H is transferred in the present hydrogen migration step, and therefore, we think the use of the PCET term is justified here (for details of population analysis, see the Supporting Information).

(21) The identity of the catalyst resting state (i.e., the turnover-determining intermediate—see Kozuch, S.; Shaik, S. *Acc. Chem. Res.* **2011**, *44*, 101) is uncertain. In the KIE calculations, it was assumed that the resting state does not involve **2a** as the ligand. For more details about the KIE calculations, see the Supporting Information.

(22) Anslyn, E. V.; Dougherty, D. A. *Modern Physical Organic Chemistry*; University Science Books: Herndon, VA, 2006; pp 435−437. ISBN 1-891389-31-9.

(23) (a) Diao, T.; Stahl, S. S. *J. Am. Chem. Soc.* **2011**, *133*, 14566. (b) Diao, T.; Pun, D.; Stahl, S. S. *J. Am. Chem. Soc.* **2013**, *135*, 8205.

(24) The system studied herein is different to the scenarios discussed in ref 12b. In the fifth scenario of this paper, the absence of KIE in an intramolecular competition experiment is attributed to the reversibility of the C−H bond cleavage step because in this particular example, the C−H and C−D bonds would otherwise be equally accessible in the product-determining step. This is not the case in this mechanistic scenario.

(25) For accounts describing the scope of α-arylation with α-dicarbonyl compounds, see (a) Kawatsura, M.; Hartwig, J. F. *J. Am. Chem. Soc.* **1999**, *121*, 1473. (b) Fox, J. M.; Huang, X.; Chieffi, A.; Buchwald, S. L. *J. Am. Chem. Soc.* **2000**, *122*, 1360 For a discussion of ligand effects on α-arylation of β-dicarbonyl compounds, see: ref 17c. The authors propose that bulky ligands assist in the reductive elimination step, but no mention is made of the ligand effects on the tautomerization step.

(26) For a review on base-induced concerted metalation-deprotonation mechanism, see (a) Ackermann, L. *Chem. Rev.* **2011**, *111*, 1314. See also (b) Gorelsky, S. I.; Lapointe, D.; Fagnou, K. *J. Am. Chem. Soc.* **2008**, *130*, 10848. (c) Biswas, B.; Sugimoto, M.; Sakaki, S. *Organometallics* **2000**, *19*, 3895.

(27) Aikawa, K.; Honda, K.; Mimura, S.; Mikami, K. *Tetrahedron Lett.* **2011**, *52*, 6682.

(28) We cannot rule out the involvement of dinuclear Pd(II) species in the C-C bond forming process. For an example of palladation in a dinuclear Pd(II) species, see Sanhueza, I. A.; Wagner, A. M.; Sanford, M. S.; Schoenebeck, F. *Chem. Sci.* **2013**, *4*, 2767.

(29) In addition to **5**, addition of DMPU also increases the overall reaction rate (rate$_{max}$ = 2.0 mM min^{-1} for **3a** with 50 mol% of DMPU vs 1.7 mM min^{-1} under the standard conditions).

(30) Corey, E. J.; Ensley, H. E. *J. Am. Chem. Soc.* **1975**, *97*, 6908.

(31) The diastereoselective version also tolerates cyclic 6-membered β-keto esters, but the products could not be obtained in pure form.

(32) The absolute stereochemistry of the products was determined by X-ray analysis of **3aj**. Other products were assigned by analogy. See the Supporting Information for details.